J Mol Model (2013) 19:65–71
DOI 10.1007/s00894-012-1523-z

ORIGINAL PAPER

Rectifying behavior of charge transfer complexes of tetrakis (dimethylamino)ethene with acceptor molecules: a theoretical study

Serguei Fomine

Received: 12 April 2012 / Accepted: 28 June 2012 / Published online: 15 July 2012

Abstract The effect of electric field induced electron transfer on the rectification properties of molecular rectifiers based on charge transfer complexes of tetrakis(dimethylamino)ethane (TDAE) with acceptor molecules was explored. The current–voltage curves and the rectification ratios (RR) for two different molecular rectifiers were obtained using a direct ab initio method at M06/LACVP (d) level of theory in the range from −2 to +2 *V*. The highest RR of 25.7 was determined for the complex of TDAE with 2-nitropyrene-4,5,9,10-tetraone at 0.5 *V* (**D1**), while another rectifier [complex of TDAE with 2,7-dimethyl nitropyrene-4,5,9,10-tetraone (**D2**)] showed a maximum RR of only 2.9 at 0.3 *V*. The electric field induced electron transfer occurring in **D1** creates a one-way conducting channel consisting of two SOMOs involving the entire **D1** complex. In the case of **D2**, no electron transfer occurs at the applied bias voltages due to the relatively high energy difference between HOMO and LUMO.

Keywords Molecular rectifier · DFT · Charge transfer · Tetraaminoethylene

Introduction

In recent years, molecular electronics have been considered as one of the most promising alternatives for future nanoscaled electronic devices [1–4]. Nowadays a great variety of potentially useful molecular electronic devices, such as molecular rectifiers, resonant tunneling diodes, wires and storage devices, have been designed and studied at both experimental and theoretical level [5–10]. The first design of a molecular rectifier is dated 1974, when Aviram and Ratner [11] proposed a prototype of a donor-insulator-acceptor (D-B-A) molecular rectifier, with functionality similar to *p-n* junctions. In D-B-A molecular diodes, D and A are the π donor and π acceptor, respectively, separated by an insulating sigma bridge (B).

The rectifying effect in molecular junctions of the form metal|molecule|metal, is defined in terms of the absence of inversion symmetry, $I(V) \neq -I(-V)$, where I and V are the current and the applied voltage, respectively. The dominant factors inducing rectification are geometric asymmetry in the molecular junction and the spatial profile of the electrostatic potential [12, 13].

Many different molecules exhibiting rectifying effect have been designed, synthesized and studied in recent years [14–16]. The rectifying behavior of D–B–A diodes in Langmuir–Blodgett (LB) layers and in dyad chromophores aligned by self-assembly have also been investigated [14, 17–26]. Recently, molecular diodes have been obtained by the assembly of ionic acceptors and donors, yielding a rectification ratio (RR) of 100 at 1 *V* [27]. Rectification behavior has also been observed in derivatives of fullerene[60] acting as a super-rectifier when operated between +2 to −2 *V* with a RR=20,000 at 1.5 *V* [28–30]. Electrical rectification from a fullerene[60]-dyad based metal–organic–metal junction of a monolayer LB film of a fullerene C60-didodecyloxybenzene dyad sandwiched between two gold electrodes was found to be as high as 158 at 3 *V* [31].

Recently, a new approach to the design of a molecular rectifier has been proposed by García et al. [32] consisting of the use of donor-acceptor complexes as molecular rectifiers. Thus, for complexes of C60 with various organic donors, RR values of up to 74 at 0.3 *V* have been estimated. It has been shown that the asymmetric evolution and

S. Fomine (✉)
Instituto de Investigaciones en Materiales,
Universidad Nacional Autónoma de México,
Apartado Postal 70-360, CU, Coyoacán,
Mexico DF 04510, Mexico
e-mail: fomine@servidor.unam.mx

alignment of molecular orbitals with the applied bias is essential in generating the molecular diode rectification behavior. If the energy difference between the HOMO of the donor and LUMO of acceptor is small enough, then the applied bias voltage is able to invert their relative energies, causing electron transfer from donor to acceptor molecule (Fig. 1) generating a biradical state. On the other hand, the opposite bias voltage will result in an increased HOMO–LUMO gap, leaving intact the electronic structure of charge transfer (CT) complex The goal of this paper was to investigate the importance of this effect on the rectification properties of such CT complexes.

Computational details

All calculations were carried out using the Gaussian 09 suit of programs [33] with the M06 [34] functional and 6-31G(d) basis set for all except gold atoms; the LANL2DZ pseudopotential basis set was used to model gold atoms of the electrodes—this basis set is denominated as LACVP(d). M06 functional was shown to produce excellent results for weakly bound and transition metal complexes [35].

The choice of donor and acceptor components was determined by their HOMO–LUMO energy gap, calculated at M06/6-31G(d) level of theory. Tetrakis(dimethylamino)ethene (TDAE) was selected as a donor molecule since tetraaminoethylene derivatives are known to be one of the best organic donors [36] and it is known that TDAE forms an ion-radical salt easily with C60 [37]. The derivatives of a known organic acceptor pyrene-4,5,9,10-tetraone; 2,7-dimethylpyrene-4,5,9,10-tetraone (DMPTO) and 2-nitropyrene-4,5,9,10-tetraone (NPTO) were selected as the acceptor part of the devices (Fig. 2).

The LUMO energies of DMPTO and NPTO are −3.235 and −3.900 eV, respectively, while the HOMO energy of TDAE is −4.066 eV. As can be seen, the HOMO–LUMO gap is small for those donor and acceptors making it possible to revert their relative energies when bias voltage is applied.

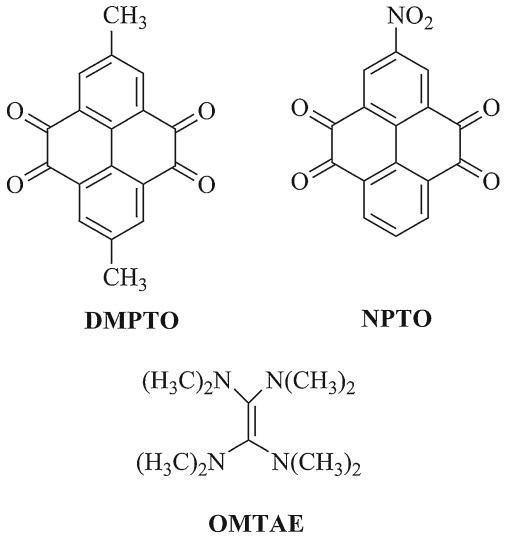

Fig. 2 Chemical structure of organic donor tetrakis(dimethylamino) ethene (TDAE) and acceptors pyrene-4,5,9,10-tetraone; 2,7-dimethylpyrene-4,5,9,10-tetraone (DMPTO) and 2-nitropyrene-4,5,9,10-tetraone (NPTO) of the studied CT complexes

To calculate *I-V* curves for CT complexes, the following computational setup was used (Fig. 3).

Electrodes are represented by a fragment of an Au(111) surface containing six atoms, located parallel to the donor and acceptor planes. It has been shown that representing the electrode by six Au atoms is sufficient to produce results reasonably close to experimental values [38]. First, the CT complex is fully optimized without any symmetry constraints. Then, electrodes are placed and the total system is optimized with the CT complex frozen. The last step involves optimization of the electrode-complex-electrode system with frozen metal atoms leaving atoms of CT complex unfrozen. The calculation of *I-V* curves was carried out

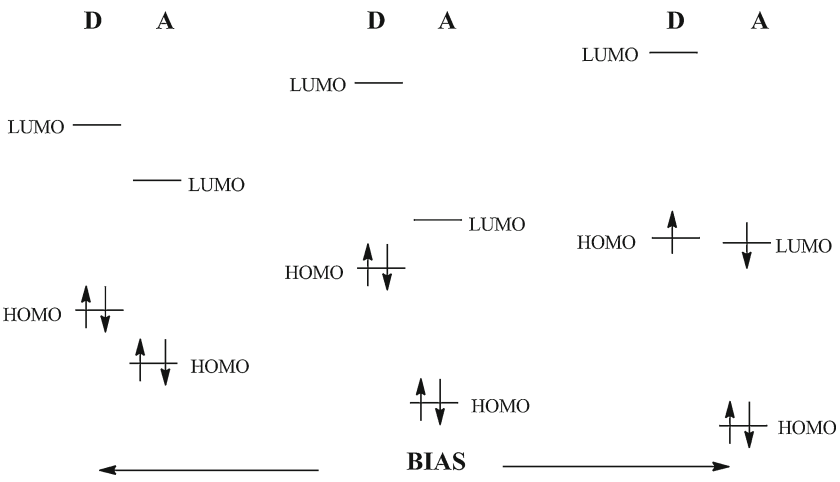

Fig. 1 Evolution of molecular orbitals of charge transfer (CT) complexes on applied bias voltage

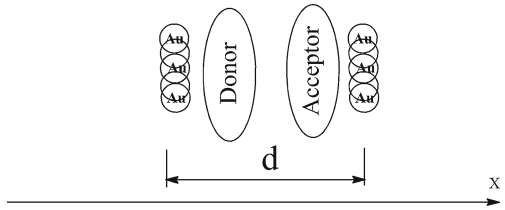

Fig. 3 Computational setup of a molecular rectifier based on a CT complex

using a direct fully ab initio method described in detail elsewhere [38, 39]. This method reproduces well experimental finding at low bias voltage (0–2 V). The current (I) is calculated according to the following equation:

$$I = \frac{2\Delta Q \Delta E}{h} \quad (1)$$

Where ΔQ is the charge difference at the electrode, before and after applied voltage, and $\Delta E = E_0 - E_v$, where E_0 is the total electronic energy the system under study without applied electric field and E_v is the total electronic energy with applied electric field. Mulliken charges for individual atoms at right electrode were used to calculate ΔQ. The rectification ratio (RR) is calculated as $I(-V)/I(V)$, where $I(-V)$ is electric current under voltage $-V$ and $I(V)$ is electric current under voltage V.

It has been shown that unrestricted DFT (UDFT) performs surprisingly well in the case of singlet biradicals [40, 41]. UDFT results obtained for the ground state of oligoacenes were in excellent agreement with CASSCF calculations [42]. UDFT leads to symmetry breaking of the Kohn-Sham ground state of singlet biradical because of a mixing of the ground state with the lowest triplet state. Therefore, a broken-symmetry (BS) UDFT approach was selected to describe the ion-radical salt formed after the electron transfer from donor to acceptor. To generate the BS solution, guess=mix keyword was used. It has been shown that BS UDFT is adequate to describe the open-shell singlet state provided the overlap between the open shell orbitals is small, which is the case for ion-radical salts formed by electron transfer from donor to acceptor [43]. Additionally CASSCF (6,6)/6-31G(d)//M06/6-31G(d) calculations on CT complexes were carried out for comparison with BS-UDFT data.

Results and discussion

Properties of CT complexes at zero bias

DMPTO and NPTO both form CT complexes with TDAE. The optimized geometries of the complexes are shown in the Fig. 4.

The complex binding energy estimated at M06/6-31G(d) level of theory was found to be of 9.0 and 1.8 kcal mol^{-1} for NPTO–TDAE and DMPTO–TDAE, respectively. Such small binding energies considering the strong electron donor properties of TDAE are due to bulky dimethylamine substituents impeding close contact and efficient overlapping of π orbitals of donor and acceptor which is of importance for good rectification properties [32]. Thus, the distance between the plane of acceptor molecules and the olefin bond of TDAE are of 4.48 and 4.21 Å, respectively, which is

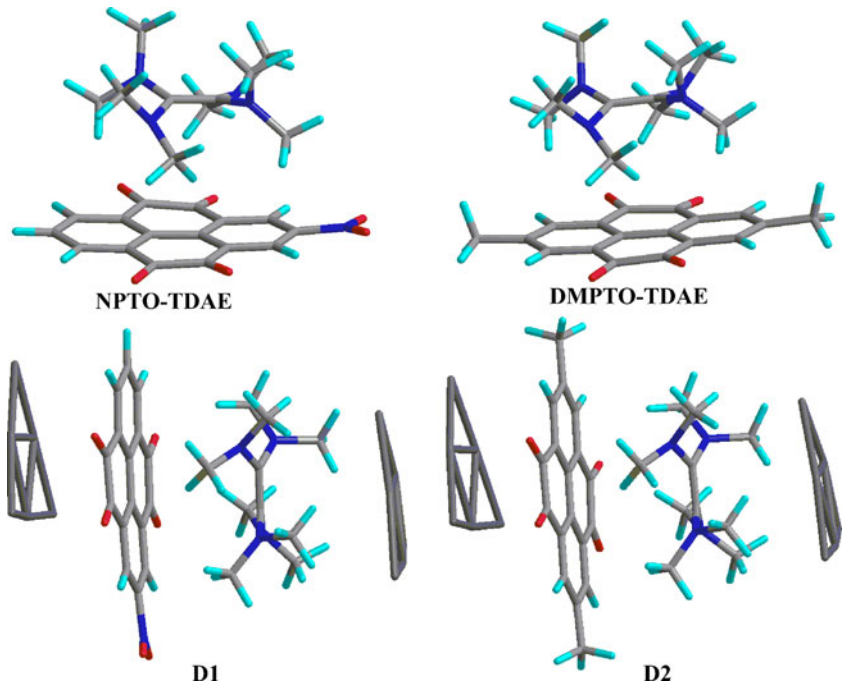

Fig. 4 M06/LACVP(d) optimized geometries of CT complexes and corresponding molecular rectifiers

larger than the sum of Van der Waals radii of carbon atoms. The lengths of the olefin bond in TDAE and the corresponding complexes are practically the same (1.362 Å), and reasonably close to the experimental data reported for TDAE (1.38 Å) [36]. The higher binding energy of the NPTO–TDAE complex is related to the lower LUMO of NPTO compared to DMTO; there is a direct correlation between the binding energy of CT complexes and the difference between ionization potential and the electron affinity of their donor and acceptor components, respectively [44]. The Mulliken charges at donor moieties are close to 0, at 0.04 and −0.05 electron, respectively. Therefore, the binding in CT complexes NPTO–TDAE and DMPTO–TDAE is mostly Van der Waals in nature with little contribution from charge transfer.

Properties of CT complexes at applied bias voltage

When bias voltage is applied perpendicular to the CT complex plane, the behavior of the two complexes is quite different. In the case of DMPTO–TDAE, the voltage applied in the range from −2 to +2 *V* causes little change as can be seen in Figs. 5 and 6.

The Mulliken charges at the donor atom change in the range from −0.01 to 0.06 while the olefin C=C bond does not change its length in the range of the applied voltage. On the other hand, while the positive bias voltage does not produce noticeable changes in NPTO–TDAE complex (Figs. 5, 6), the negative bias does. As seen from Figs. 5 and 6, starting from −0.33 *V* there is a strong increase in positive charge at the donor. Thus, in the range of bias from −0.27 to 0.67 *V*, the positive charge at the donor atom increases from 0.07 to 0.8 electrons. Simultaneously, the olefin C=C bond of TDAE is elongated from 1.36 to 1.42 Å. At the same time, starting from −0.33 *V*, the restricted solution

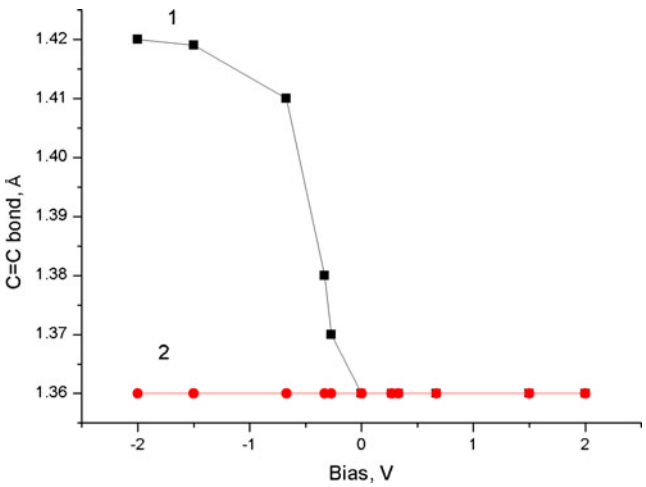

Fig. 5 Evolution of C=C TDAE bond on applied bias voltage in NPTO-TDAE (*1*) and DMPTO-TDAE (*2*) CT complexes

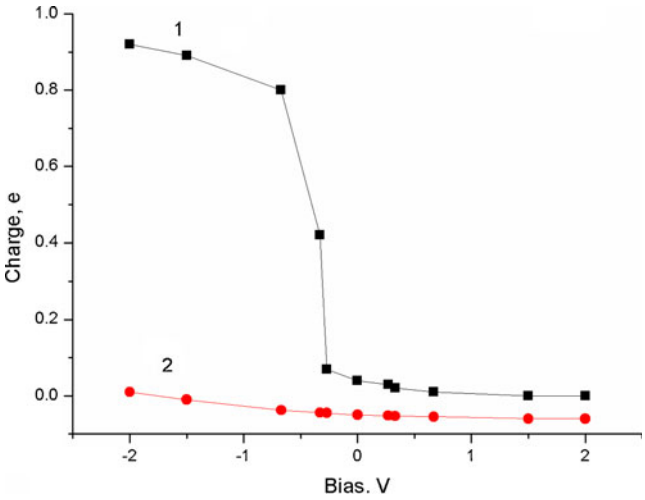

Fig. 6 Evolution of Mulliken charges at the TDAE fragment on applied bias voltage in NPTO–TDAE (*1*) and DMPTO–TDAE (*2*) CT complexes

is no longer stable for the complex. The unrestricted solution becomes the stable one for the NPTO–TDAE complex for biases more negative than −0.33 *V*, suggesting the biradical character of the ground state. Thus, the $<S^2>$ for biases of −0.33, −0.67, −1.5 and −2.0 *V* are of 0.43, 0.88, 0.99 and 1.01. The $<S^2>$ for pure biradical is exactly 1, representing a 50 % mixture of singlet and 50 % of triplet states. Therefore, the electronic structure of NPTO–TDAE is a pure biradical state for biases more negative than −0.67 *V* due to electron transfer from HOMO of the donor to the LUMO of the acceptor according to Fig. 1. The HOMO of TDAE and LUMO of NPTO are shown in Fig. 7 As can be seen, the most important contribution to HOMO comes from bonding π orbitals of the C=C bond, thus explaining the increase in bond length as the electron transfer proceeds. The complete electron transfer from donor to acceptor also confirms CASSCF(6,6) calculations for the NPTO-TDAE complex at −2 *V* bias voltage when exactly two electrons are found outside the valence shell, which is in line with $<S^2>$ for pure biradicals.

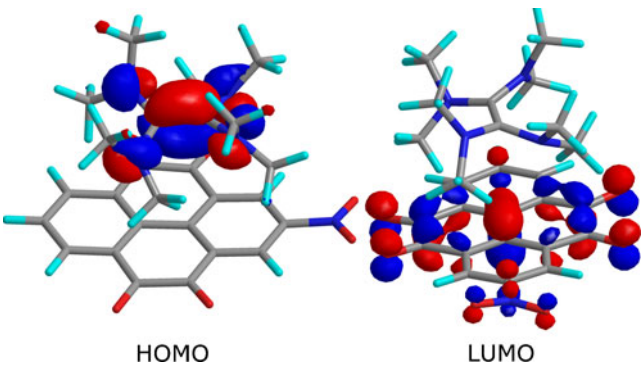

Fig. 7 HOMO and LUMO in NPTO–TDAE at zero bias voltage

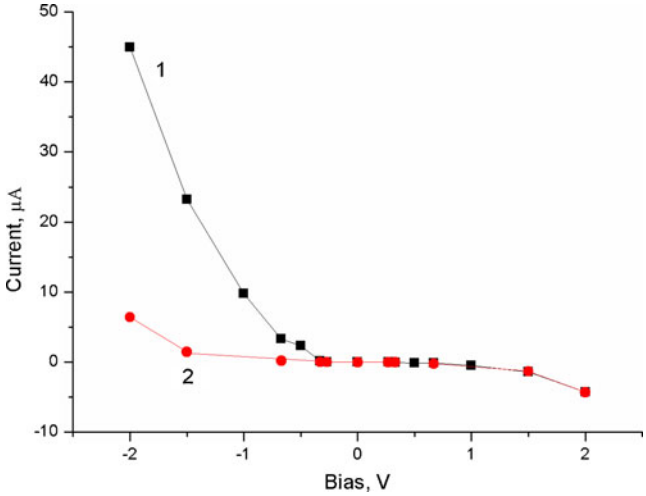

Fig.8 Current–voltage characteristics for molecular rectifiers **D1** (*1*) and **D2** (*2*)

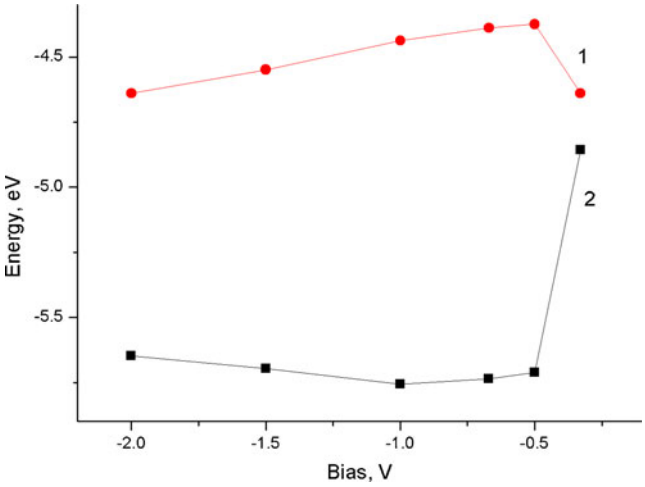

Fig. 10 Evolution of α-SOMO (*1*) and β-SOMO (*2*) energies for **D1** with bias voltage

Rectification behavior of molecular diodes D1 and D2

Figures 8 and 9 show *V-I* curves and RRs at different bias voltages for diodes **D1** and **D2**, respectively. As can be seen, there are strong differences between them. In case of **D1**, RR increases from 0 to 0.5 V showing a maximum of about 25. After that, RR decreases slowly to around 11 for a bias of 2 V.

For **D2**, however, RR does not exceed 3 in the range from 0 to 2 *V*. This difference is related to the relative energies of HOMO and LUMO for diodes **D1** and **D2**. Thus, **D1** and **D2** behave similarly at positive biases (Fig. 8) where the current changes from 0 to 4.3 μA for both diodes in the range from 0 to 2 *V*. The HOMO–LUMO gap increases slowly from 0.91 to 1.21 eV for **D1** and from 1.22 to 1.24 eV for **D2**, respectively. The situation changes at negative bias (Fig. 10). Similar to the corresponding **CT** complex, starting from −0.3 *V*, the restricted solution is no longer the lowest energy state for **D1** due to electron transfer from donor to acceptor, and HOMO and LUMO become SOMOs with very close energies (with a difference of 0.21 eV at −0.33 *V*). The ground state becomes multiconfigurational for bias voltage more negative than −0.27 *V*. Thus, the biradical state is created as follows from the $<S^2>$ value, which increases from 0.13 for −0.33 *V* to 1.02 for −2 *V*. These close lying SOMOs create a conductive channel in **D1** when negative bias is applied. On the other hand, such a mechanism does not exist for positive bias where the HOMO–LUMO gap increases with voltage and no electron transfer is possible. In the case of **D2**, the applied negative bias is not sufficient to cause electron transfer from donor to acceptor and create SOMOs due to the higher lying LUMO; therefore, the electronic structure of **D2** is not very different for the positive and negative biases, resulting in low RR in the selected range of voltages. Figure 11 shows the α-SOMO and β-SOMO for a bias voltage of 0.5 *V* where maximum RR is

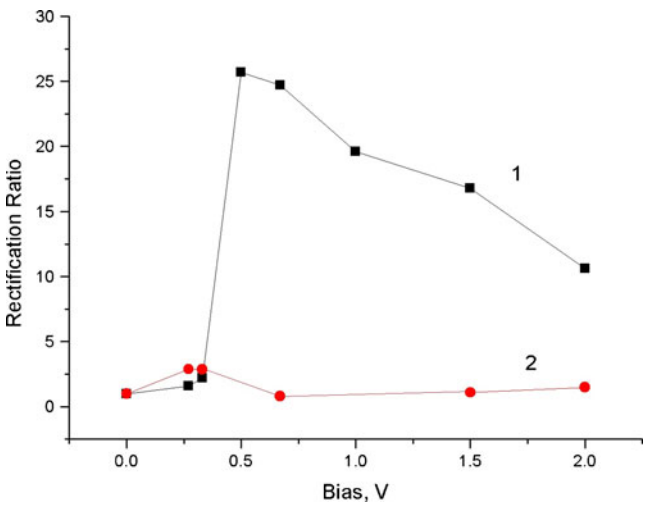

Fig. 9 Rectification ratios (RRs) of molecular rectifiers **D1** (*1*) and **D2** (*2*)

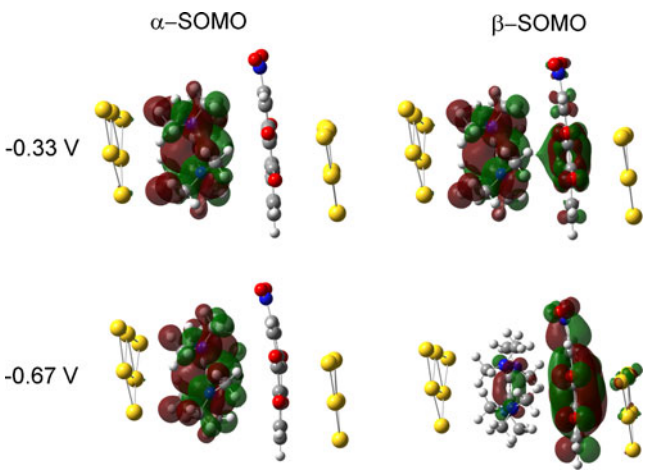

Fig. 11 α-SOMO and β-SOMO of **D1** at biases of −0.33 and −0.67 *V*

estimated. As can be seen, they extend over the entire **D1**, thus facilitating electron transport.

After achieving maximum RR of about 25 at −0.5 V, RR starts to decrease, reaching 10.6 at −2.0 V for **D1**. This is attributed to the following phenomenon: when HOMO and LUMO energy splitting decreases enough in response to the applied bias, electron transfer from HOMO to LUMO creates α- and β- SOMOs in a biradical state. The electron transfer rate can be estimated from $<S^2>$, which is 0 when no electron transfer occurs and 1 when electron transfer is complete (biradical state). Thus $<S^2>$ for **D1** is 0.13, 0.96, 0.97, 1.0, 1.0, and 1.0 for biases of −0.33, −0.50, −0.67, −1.0, −1.5, and −2.0 *V*, respectively. Therefore, the electron transfer process occurs between −0.33 and −0.67 V, exactly in the range where maximum RR is observed. Electron transfer transforms HOMO and LUMO into two SOMO orbitals. As the electron transfer advances, the energy of SOMO derived from HOMO declines due to a decrease in electron repulsion, while SOMO derived from LUMO increases its energy due to the opposite trend (Fig. 11). This leads to an increase of the energy splitting between SOMOs and, as a result, in a decrease of the conductive channel efficiency. On the other hand, as the electron transfer proceeds, two SOMO orbitals expand over **D1**, favoring conductivity (Fig. 11). Those two opposite trends cause the appearance of a maximum on the RR curve of **D1**.

Conclusions

The calculations presented here demonstrated that reversible electric field induced electron transfer from donor to acceptor to form a biradical state favors the rectification properties of CT complexes due to formation of a conductive channel in the biradical state consisting of two SOMOs extending over the entire CT complex. The electric field induced biradical state is formed when HOMO of donor and LUMO of acceptor are close enough in energy, and when the electric field vector is perpendicular to the CT plane pointing from donor to acceptor. When the electric field vector is in the opposite direction, no electron transfer occurs and, therefore, no biradical state is formed. Two molecular diodes, **D1** and **D2**, based on a TDAE donor molecule and NPTO and DMPTO acceptors, respectively, were studied. The electron transfer from TDAE to NPTO in **D1** starts at 0.33 *V*, resulting in nearly complete electron transfer from donor to acceptor at 1 *V*. The maximum RR of 25.7 is estimated for **D1** at 0.5 *V*. In **D2**, no electron transfer occurs in the range of voltages studied due to higher HOMO–LUMO energy differences, and the maximum RR of only 2.9 was estimated for bias of about 0.3 *V*. Therefore, the phenomenon of reversible electric field induced electron transfer in CT complexes can be applied to the design of new types of molecular rectifiers.

Acknowledgment This research was carried out with the support of Grant 151277 from National Council for Science and Technology (CONACyT)

References

1. Kubatkin S, Danilov A, Hjort M, Cornil J, Brédas JL, Stuhr-Hansen N, Hedegård P, Bjórnholm T (2003) Nature 425:698–701
2. Yu LH, Natelson D (2004) Nano Lett 4:79–83
3. Dadosh T, Gordin Y, Krahne R, Khivrich I, Mahalu D, Frydman V, Sperling J, Yacoby A, Bar-Joseph I (2005) Nature 436:667–680
4. Song H, Kim Y, Jang YH, Jeong H, Reed MA, Lee T (2009) Nature 462:1039–1043
5. Tour JM (2000) Acc Chem Res 33:791–804
6. Carroll RL, Gorman CB (2002) Angew Chem Int Ed 41:4378–4400
7. Seminario JM, Zacarias AG, Tour JM (2000) J Am Chem Soc 122:3015–3020
8. Brandbyge M, Mozos JL, Ordejón P, Taylor J, Stokbro K (2002) Phys Rev B 65:165401
9. Soler JM, Artacho E, Gale JD, García A, Junquera J, Ordejón P, Sánchez-Portal D (2002) J Phys Condens Matter 14:2745–2779
10. Taylor J, Guo H, Wang J (2001) Phys Rev B 63:245407
11. Aviram A, Ratner MA (1974) Chem Phys Lett 29:277–283
12. Mujica V, Ratner MA, Nitzan A (2002) Chem Phys 281:147–150
13. Stokbro K, Taylor J, Brandbyge M (2003) J Am Chem Soc 125:3674–3675
14. Ng MK, Lee DC, Yu LP (2002) J Am Chem Soc 124:11862–11863
15. Ng MK, Yu LP (2002) Angew Chem Int Ed Engl 41:3598–3601
16. Elbing M, Ochs R, Koentopp M, Fischer M, Hanisch CV, Weigend F, Evers F, Weber HB, Mayor M (2005) Proc Natl Acad Sci USA 102:8815–8820
17. Metzger RM, Chen B, Hopfner U, Lakshmikantham MV, Vuillaume D, Kawai T, Wu X, Tachibana H, Hughes TV, Sakurai H, Baldwin W, Hosch C, Cava MP, Brehmer L, Ashwell GJ (1997) J Am Chem Soc 119:10455–10466
18. Martinand AS, Sambles JR (1996) Nanotechnology 7:401–405
19. Metzger RM (1999) Acc Chem Res 32:950–957
20. Metzger RM, Xuand T, Peterson IR (2001) J Phys Chem B 105:7280–7290
21. Ashwell GJ, Robinson BJ, Amiri MA, Locatelli D, Quici S, Roberto D (2005) J Mater Chem 15:4203–4205
22. Ashwell GJ, Mohib A, Miller JR (2005) J Mater Chem 15:1160–1166
23. Ashwell GJ, Chwialkowska A, High LRH (2004) J Mater Chem 14:2848–2851
24. Ashwell GJ, Chwialkowska A, High LRH (2004) J Mater Chem 14:2389–2394
25. Ashwell GJ, Hamilton R, High LRH (2003) J Mater Chem 13:1501–1503
26. Jiang P, Morales GM, Youand W, Yu LP (2004) Angew Chem Int Ed 43:4471–4475
27. Ashwell GJ, Ewington J, Robinson BJ (2006) Chem Commun 6:618–620
28. Metzger RM, Baldwin JW, Shumate WJ, Peterson IR, Mani P, Mankey GJ, Morris T, Szulczewski G, Bosi S, Prato M, Comito V, Rubin Y (2003) J Phys Chem B 107:1021–1027
29. Honiuc A, Jaiswal A, Gong A, Ashworth K, Spangler CW, Peterson IR, Dalton LR, Metzger RM (2005) J Phys Chem B 109:857–871
30. Metzger RM (2003) Chem Rev 103:3803–3834
31. Shankara Gayathri S, Patnaik A (2006) Chem Commun 18:1977–1979

32. García M, Guadarrama P, Ramos E, Fomine S (2011) Synthetic Met 21–22:2390–2396
33. Frisch MJ et al (2010) Gaussian 09, Revision B.01. Gaussian, Wallingford
34. Zhao Y, Truhlar DG (2006) J Chem Phys 125:194101
35. Zhao Y, Truhlar DG (2008) Theor Chem Acc 120:215–241
36. Bock H, Borrmann H, Havlas Z, Oberhammer H, Ruppert K, Simon A (1991) Angew Chem Int Ed Engl 30:1678–1681
37. Tanaka K, Zakhidov AA, Yoshizawa K, Okahara K, Yamabe T (1993) Phys Rev B 47:7554–7559
38. Ortiz DO, Seminario JM (2007) J Chem Phys 127:111106
39. Seminario JM, Zacarias AG, Tour JM (1999) J Phys Chem A 103:7883–7887
40. Marquardt R, Balster A, Sander W, Kraka E, Cremer D, Radziszewiski JG (1998) Angew Chem 37:955–958
41. Gräfenstein J, Hjerpe AM, Kraka E, Cremer D (2000) J Phys Chem A 104:1748–1761
42. Bendikov M, Duong HM, Starkey K, Houk KN, Carter EA, Wudl F (2004) J Am Chem Soc 126:7416–7417
43. Gräfenstein J, Kraka E, Filatov M, Cremer D (2002) Int J Mol Sci 3:360–394
44. Kost D, Frailich M (1997) J Mol Struct (THEOCHEM) 398–399:265–274